

Green Chemistry

Accepted Manuscript



This is an *Accepted Manuscript*, which has been through the Royal Society of Chemistry peer review process and has been accepted for publication.

Accepted Manuscripts are published online shortly after acceptance, before technical editing, formatting and proof reading. Using this free service, authors can make their results available to the community, in citable form, before we publish the edited article. We will replace this *Accepted Manuscript* with the edited and formatted *Advance Article* as soon as it is available.

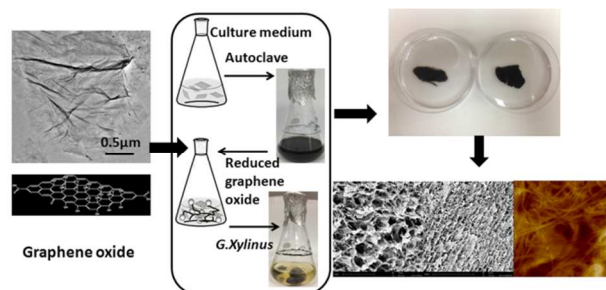
You can find more information about *Accepted Manuscripts* in the [Information for Authors](#).

Please note that technical editing may introduce minor changes to the text and/or graphics, which may alter content. The journal's standard [Terms & Conditions](#) and the [Ethical guidelines](#) still apply. In no event shall the Royal Society of Chemistry be held responsible for any errors or omissions in this *Accepted Manuscript* or any consequences arising from the use of any information it contains.



www.rsc.org/greenchem

Graphene oxide was successfully reduced to graphene using a bacterial cellulose culture medium that was further processed to fabricate *in-situ* composites of bacterial cellulose/reduced graphene oxide gelatinous hybrids, aerogels, and membranes.



Cite this: DOI: 10.1039/c0xx00000x

www.rsc.org/xxxxxx

ARTICLE TYPE

A one-pot biosynthesis of reduced graphene oxide (RGO)/bacterial cellulose (BC) nanocomposites

Avinav G. Nandgaonkar^a, Qingqing Wang^b, Kun Fu^b, Wendy E. Krause^a, Qufu Wei^b, Russel Gorga^a, and Lucian^{*b}

Received (in XXX, XXX) Xth XXXXXXXXX 20XX, Accepted Xth XXXXXXXXX 20XX
DOI: 10.1039/b000000x

Here, we report for the first time a one-pot *in-situ* biosynthetic method to fabricate structurally controllable bacterial cellulose (BC)/reduced graphene oxide (RGO) composites. The graphene oxide (GO) was highly reduced during a standard autoclave process using a traditional mannitol culture medium as the reducing agent. The RGO sheets prepared exhibits a high carbon to oxygen ratio of 3.1 as compared 1.8 for GO determined by X-ray photoelectron spectroscopy. The electrical conductivity of the RGO was found to be 23.75 S m⁻¹. The final BC/RGO composites were developed in three distinct forms: sealed structures in the water, aerogels characterized by a porous cross section and aligned longitudinal structure, and films embedded within the RGO sheets. Because of the simplicity and non-toxic nature of this work, this process can be used in biomedical and bioelectronics applications, which can be placed within the context of novel biocompatible materials.

Graphene, a reduced chemical form of graphene oxide (GO), consists of carbon atoms arranged in a single sheet-like layer that is best characterized as a honeycomb structure.¹ Graphene has gained a tremendous amount of recent research and societal notoriety because of its unique electrical, thermal, and mechanical properties. A number of efforts have attempted to utilize it in preparing aerogels for super capacitance,² light and flexible conductors,^{3,4} and photoconductors of nitrogen and oxygen gases.⁵ A significant amount of research time has been expended recently in targeting the reduction of GO. Different methods have been utilized to reduce GO and functionalize it which includes among the following: hydrothermal reduction,⁶ electrochemical vapor deposition,^{3,7} photochemical reduction,⁸ burn-quench method,⁹ and chemical reduction.⁴ However, the latter methods typically involve the need for expensive equipment; tend to be complicated processes to implement; utilize hazardous chemicals; involve a long reducing time; and necessitate high temperatures, all of which are not environmentally sustainable, nor suitable for large scale industrial production. Numerous "green" methods have been investigated to reduce GO which could be more advantageous than other methods for its future production. Biocompounds such as amino acids,¹⁰ vitamin C,¹¹ BSA (bovine serum albumin),¹² lysozyme,¹³ and green tea¹⁴ have all been used as reducing agents for GO.

These products are quite safe and non-toxic as compared to hydrazine and other chemical reducing agents; however, several of these reducing agents can require one day or longer for a useful reduction of GO. Therefore, a simple and more environmentally friendly process is needed to reduced GO which can be embedded *in-situ* to prepare bacterial cellulose ("vinegar" bacteria produce nano-cellulose) graphene composite during the culturation period which had added advantage of biocompatibility and cost efficiency for various applications.

A green, economical, and scalable process for the fabrication of aerogels can developed by utilizing bacterial cellulose, a natural biomaterial which as a general material (in trees and plants as well) is the world's most abundant renewable material. Bacterial cellulose (BC) is produced from various species of bacteria such as *Gluconacetobacter xylinus*. Due to cellulose's high water uptake capacity, it has the tendency to form gels. It possesses high tensile strength, biocompatibility, and purity. BC has found various applications in fields such as paper and paper-based products, audio components, and soft tissue engineering.¹⁵ Apart from these applications, BC has also been widely used for highly conductive and stretchable conductors,¹⁷ lithium ion battery anodes,¹⁸ conductive and pressure sensing aerogels,¹⁹ and fire-resistant aerogels.²⁰ However, these methods are not straightforward to apply because they require additional time-consuming, energy-intensive, or expensive steps such as pyrolyzation at very high temperatures, the application of curing agents, or chemical modification at the very least. Post treatments have been carried on cellulose to prepare a composite film of cellulose and reduced graphene for applications in supercapacitance²¹ and flexible and conductive films.²² *In-situ* synthesis of bacterial cellulose in conjunction with various types of reagents/nutrients/chemical additives in the culture solution has also been carried out to further exploit and enhance the final properties of bacteria cellulose. Multi-walled nanotubes (MWNT), for example, have been incorporated inside a BC culture medium to produce composites of BC/MWNT as a biomaterial,^{23, 24} anatase nanoparticles were incorporated to form photoacatalytically active hybrids,²⁵ and silica nanoparticles were utilized to improve the elasticity and mechanical strength of bacterial cellulose.²⁶

Recently, yeast extract has been shown to act as a reducing agent,^{27, 28} biocatalyst, and mediator.^{29, 30} Because yeast extract is a nutrient component for the culturation of bacterial cellulose and

tends to be therefore rich in amino acids, it can be ideal as a reducing agent. So far, no research had been accomplished to reduce GO via yeast extract. Herein, we present a one-pot *in-situ* biosynthesis of GO utilizing yeast extract during an autoclave process. This method is an *in situ* process in which the GO was reduced and consequently attached to the 3D interconnected fibrous network of bacterial cellulose during the cultivation period.

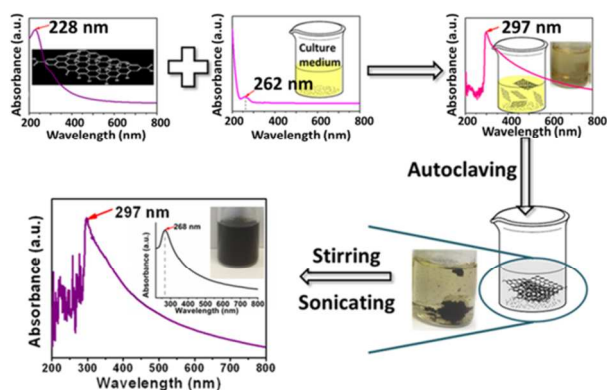


Fig. 1 A schematic illustration of the deoxygenation of graphene oxide to graphene during the autoclave process at 121°C for 15 min.

Culture medium may be defined as a cocktail of carbohydrates, proteins, peptides, amino acids, vitamins, etc., most of which have been proved to be effective reduction agents for producing RGO from GO.¹⁰⁻¹² Additionally, a hydrothermal-based process had also been reported as an environmentally friendly method to induce GO reduction.⁶ Thus, in the current process, the conditions were ideal for the reduction of GO: application of a richly reducing culture medium within a hydrothermal environment, and the combinative effects of these two processes lead to highly effective reduction of GO compared to other methods [Supplemental Information-Table S1]. Figure 1 displays an illustration of GO reduction by an autoclave process (see Methods for details). First, an aqueous solution of GO having a maximum absorption wavelength at 228 nm was added into the culture medium (maximum absorption wavelength: 262 nm). The hybrid solution demonstrated a new, strong absorption peak at 297 nm that was still extant after the autoclave process. This peak was attributed to an $n-\pi^*$ transition,¹⁰ while the strong intensity of this peak indicated that approximately 3-5 conjugated π bonds were in this newly formed structure, from which it can be conjectured that several amino acids from the yeast extract may have engaged in $\pi-\pi$ interactions with the graphene sheet.^{11, 12, 31} After the autoclave process, a black precipitate of RGO was observed which could be well dispersed by stirring and sonication. After it was washed repeatedly with deionized water, the RGO showed an absorption peak at 268 nm, which is quite similar to what has been observed with reduction from hydrazine (270 nm), and relatively strong in comparison to all of the “green” reduction processes available [Supplemental Information, Table S1]. From the UV-vis spectra obtained with different autoclaving time [Supplemental Information Figure S1], it can be concluded that the reduction can be completed within 15 min, because no peak shift was observed beyond this time.

To further elucidate the reduction process witnessed, the three ingredients in the culture medium, i.e., yeast extract, mannitol,

and peptone were separately added into an aqueous solution of GO [see Supplemental Information Figure S2]. After autoclaving, the pure GO displayed a darker color, but no precipitation. Compared with the pure GO solution, the mannitol system displayed a lighter color, while the peptone had a darker color. The most notable change was noted for the yeast extract solution containing GO. After the autoclave process, black precipitation formed in the solution. Thus, at first blush, it was possible to conclude that the yeast extract played a significant role in dehydration of GO.

The yeast extract is known to be comprised of a cocktail of protein/polypeptides, amino acids, carbohydrates, vitamins, etc.²⁸ However, a detailed composition of the yeast extract is not so easily gleanable. Thus, the mechanism has not been fully explored and understood at this time and will certainly require further investigation. However, yeast extract is typically recognized by the biochemical community as a combination of reduction agent,^{27, 28} stabilizer,¹¹ as well as redox mediator.³² In the current hydrothermal process, water behaves as a strong electrolytic medium, having a high diffusion coefficient and dielectric constants, which allows the catalysis of a variety of reactions that involve heterolytic bond cleavage and thus facilitating the removal of oxygen groups via dehydration reactions.³³

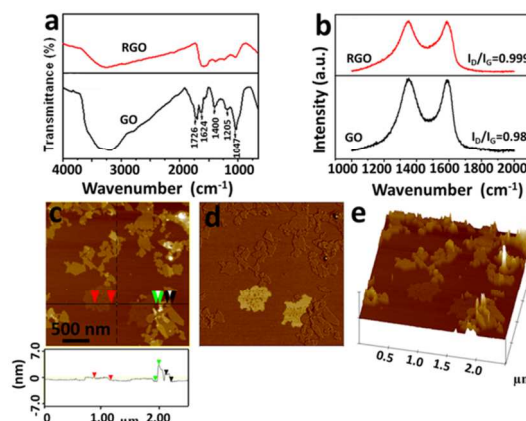


Fig. 2 Characterization of GO and RGO. (a) FTIR spectra & (b) Raman spectra of GO before and after reduction. (c) AFM topography and cross-section (d) phase (e) corresponding 3D topography images of RGO.

The RGO was characterized by FTIR to confirm changes in its chemical structure before and after deoxygenation. As shown in Figure 2 (a), the GO showed a strong and broad band at 3000-3500 cm^{-1} , which can be assigned to the stretching vibration of hydroxyl groups. The peak at 1724 cm^{-1} is attributed to the classical C=O stretching vibration of carboxylic acid. The characteristic peaks at 1205 cm^{-1} and 1047 cm^{-1} can be attributed to the epoxy C-O stretching vibration and the alkoxy C-O stretching vibration, respectively.³⁴ Finally, the peak at 1400 cm^{-1} is indicative of the deformation vibration of tertiary alcohol C-OH.³⁵ After reduction, the peaks for oxygen-containing groups significantly decreased or disappeared, the characteristic peak of C=C stretching vibration at 1624 cm^{-1} increased, illustrative of the removal of most oxygen-containing groups and restoration of π -conjugation.¹⁰ In addition, the FTIR spectrum of RGO possesses similar spectral features to that of Vitamin C-reduced RGO that is stabilized by L-tryptophan,¹¹ supporting the premise

that the RGO obtained in the current process may also be coated by biomolecules from the culture medium.

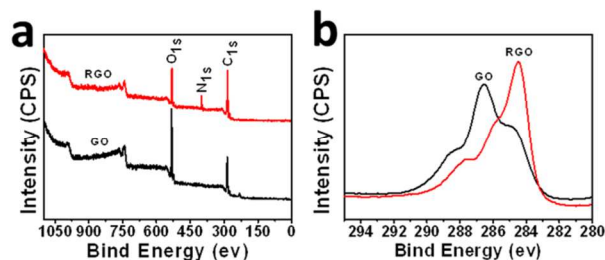


Fig. 3 XPS spectra of GO and RGO, survey scan (a), and in the region of C 1s

Table 1 Elemental composition of pure GO and RGO as determined by XPS analysis.

Sample	Carbon (at %)	Oxygen (at %)	Nitrogen (at %)	C/O ratio
Graphene Oxide (GO)	62.1	35	1.6	1.8
Reduced Graphene Oxide (RGO)	69.2	22.3	8.5	3.1

The graphene oxide reduction had been confirmed by the XPS results. Figure 3a and Table 1 show the elemental analysis of pure GO and RGO confirm the successful reduction of graphene oxide. The C/O ratio increased after the reduction process for 15 mins by using yeast extract. Furthermore, figure 3b shows the XPS spectra of pure GO and RGO in C 1s regions. The C 1s peak of GO was observed at 284.8 eV and C 1s of C-O was observed at 286.6 eV.¹¹ The change in the peak shift for pure GO and RGO were due the different chemical environment. The chemical valences did not change for the RGO. However, the intensity of the C 1s of epoxy group significantly reduced, which indicates the effective reduction of graphene oxide using yeast extract.

Micro-Raman spectroscopy was used to evaluate the quality of the RGO obtained in the current process (Figure 2b). The typical features in the Raman spectra are the G band and D band, which are respectively attributed to the E_{2g} phonon of C sp^2 atoms and the breathing mode of k-point phonons of A_{1g} symmetry.³⁶ A prominent D band is indicative of a decrease in the average size of in-plane sp^2 domain of the GO or RGO,³⁷ originating from defects associated with vacancies, grain boundaries, and amorphous carbon species.⁶ The intensity ratio (I_D/I_G) of D band to G band of the GO was about 0.98. After reduction, the intensity ratio slightly increased to 0.999. This event indicates the presence of unrepaired defects that remained after the removal of oxygen moieties. However, compared with other chemical methods [Supplemental information, Table S1], the increased intensity ratio was very low, so it can be inferred that the culture medium produces higher quality graphene nanosheets from GO with respect to defects/disorder.³⁸

AFM images of GO and RGO were taken to determine the thickness, phase change, and the topography of the samples. GO was dispersed in water, while RGO was dispersed in culture media. A droplet of these solutions were placed on mica disks

and then oven dried. Figure 2 (c-e) shows the topographic images of the as-prepared RGO and its corresponding phase and 3D images. A cross-sectional height analysis demonstrated that the thickness of RGO is different. From left to right, the Vert distances are 0.708 nm, 4.329 nm, and 1.810 nm, respectively. Because the UV-vis and FTIR had already provided compelling evidence that RGO was coated by biomolecules, different thicknesses from the current measurement can only be explained as arising from surface coatings that presumably originate from different amounts of biomolecules. Compared to the original thickness of GO (1 nm, provided by XFnano), the RGO sheet with the thickness of 0.708 nm may be treated as the blank RGO without any biomolecules coating(s), an inference that was confirmed by the phase image. Blank RGO had a higher phase than biomolecule-decorated RGO, while the corresponding 3D topographic image confirmed that the coating layer was not uniform. This type of structure will clearly contribute to a higher native biocompatibility for the RGO sheets,^{11, 12} making the *in-situ* biosynthesis of BC/RGO composites more feasible.

To examine the electrical conductivity of the RGO, the RGO sheets were pressed into a film and then tested by four-point probe instrument. From the results, the average conductivity of the RGO sheet was found about 23.75 S m^{-1} . Although, the electrical conductivity of the RGO sheet is lower than the other methods such as Vitamin C,¹¹ it is comparable with that made from other green methods.¹⁴ Therefore, it is demonstrated that the yeast extract can reduced the graphene oxide which can provide unique electrical properties. Note that the culture medium molecules are heavily adsorbed on the graphene surface which can interfere with the electrical conductivity measurements to some extent. However, considering the biocompatibility of the culture medium, the RGO functionalized with these biomolecules can be used for bioapplications.

The *Glucanacetobacter xylinus* bacterial strain can produce a gelatinous membrane (pellicle) at the air-liquid interface under static conditions.³⁹ However, it has been recommended and verified within the recent efforts of this group (manuscript sent to *Soft Matter*) that agitated conditions encourage higher cellulose yields from a practical perspective,⁴⁰ although it was discovered that the overall cellulose quantity was slightly reduced under agitated conditions.^{39, 41} In the current work, the effect of agitated conditions was studied to better understand the adsorption behavior of the reduced graphene during the growth of bacterial cellulose. Moreover, it is known that other chemical properties can be tuned under agitated conditions such as crystallinity, crystal size, and cellulose Ia content.⁴² Further studies on the absorption of RGO under static conditions are currently on going in our laboratories.

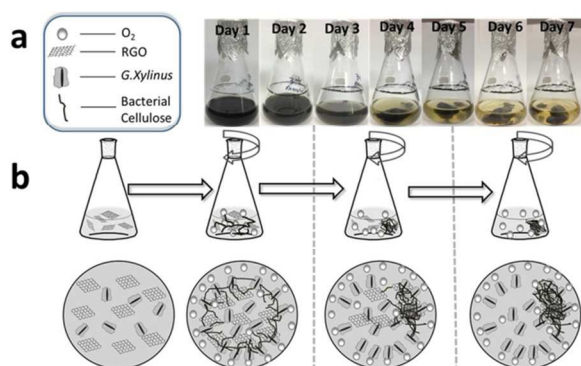


Fig. 4 Growth of bacterial cellulose in the presence of reduced graphene oxide (RGO) sheets: (a) photographic image of the 7 day track of bacterial cellulose growth in presence of RGO under agitated conditions, (b) schematic illustration of formation of bacterial cellulose and the integration of graphene sheets into the 3D interconnected fibrous network of BC.

After two cycles of stirring and sonicating, it was possible to obtain a stable dispersion of graphene in the culture solution. The culture solutions were stable even at relatively high concentrations of GO (0.5mg/mL), while the color of the culture solution was found to be jet black reflective of a homogeneous dispersion of graphene sheets. After the dispersion of the RGO in the culture medium, a two-day old bacterial cellulose culture supernatant was added into the flask. Figure 4a illustrates the bacterial cellulose growth track containing 0.1 mg/mL of RGO for 7 days. On the first day, the solution was black in color with little or no bacterial cellulose growth. As the time progressed (days 2-3), the black color solution became clearer and showed very small uneven bacterial growth under visible light. On day 4, a single black bacterial cellulose pallet was observed in the culture solution. The black color was due to the incorporation of RGO to the bacterial cellulose. From day 5-7, the culture solution became more clear (same as the original culture color), indicating the incorporation of remaining RGO to the monolithic BC pallet. A similar phenomenon was reported for BC cultured with MWNTs.^{23, 24}

The morphology changes have been analyzed by SEM to illustrate any disturbance in the fibrous arrangement of BC. The particular arrangement of BC fibrils with RGO can be explained by schematic illustration (Figure 4b). On the first day, *G. xylinus* and RGO were distributed into the culture solution. The free bacteria firstly attached to the surface of air bubbles and started to multiply and produce bacterial cellulose fibrils.⁴² As the number of bacteria increased, the BC fibrils attached to the RGO sheets creating a more compact structure. Because of the continuous agitation nature of the system, the cellulose fibrils and RGO entangled in each other and created an agglomeration that was indicative of a BC/RGO composite. Because the cellulose-forming rate is slow, the RGO absorbed on the BC fibrils; however, at the same time, bacteria gathered around the BC/RGO composite and started to produce BC fibrils. This process of absorption of RGO on the BC and formation of new BC on the existing composite was continuous until a more compact structure formed. The entire agitation culture process resulted in an irregular shaped composite with a random overlapped structure.

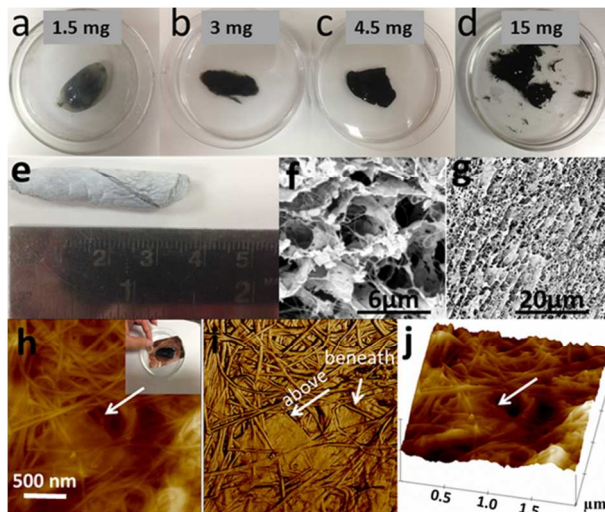


Fig. 5 The morphology of three different BC/RGO composites. (a-d) gelatinous BC/RGO composites with sealed structure. The digital images of the BC/RGO composites with increasing concentration of graphene 0.05 mg/mL (a), 0.1 mg/mL (b), 0.15 mg/mL (c), 0.5 mg/mL (d) was added into the culture medium). (e-g) BC/RGO composite aerogels. (e) The digital photograph of sample (a) after freeze drying. (f) and (g) are the representative SEM images of cross section and longitudinal structure of sample (e). (h-j) BC/RGO composite film. (h) AFM topography phase, and (j) corresponding 3D topography image.

After a cultivation period of seven days, the samples were washed by sodium hydroxide to dissolve the bacteria embedded inside the matrix of BC/RGO composite. Figure 5 (a-d) represents the digital images of never-dried gelatinous sample containing GO with increasing concentration of GO under agitated condition. The sample shown in Figure 5a contains only 0.05 mg/mL of GO and it was like a “gelatinous-packet” which had semi-transparent membranes outside covering the BC/RGO composite. This kind of structure is unique in its own way because all the RGO was encapsulated inside a thin layer of BC. This may have huge potential for diffusion-controlled release of biocompounds present on the surface of RGO through a biocompatible BC membrane. Figure 5e displays the freeze-dried sample of 5a. The outer surface contains only bacteria cellulose that had an aligned structure [see Supplemental information Figure S3-b] due to the one directional agitated motion of pellicles during cultivation. When the concentration of GO increased in the culture media, there were sufficient RGO nanosheets present that attached to the newly formed BC. Because of the agitation action and flat surface of graphene, the RGO nanosheets formed a thin membrane outside, which maintains the overall structural integrity (Figure 5b and c). All the samples had an irregular shape and the color of the samples became darker with an increase in RGO concentration. As the RGO (0.5 mg/mL) was stable in the medium before the inoculation, it was attempted to inoculate the bacteria at this high concentration. However, the BC formed in this process was not enough to adsorb all the RGO, and the as prepared BC/RGO composite was not stable and compact. Figure 5f shows the cross section and Figure 5g shows the longitudinal view of sample 5e which had a directional porosity inside the sample. The sheet-like pore structure was due to the flat surface of graphene which was connected with small interconnected BC fibrils. This showed that the RGO had been thoroughly dispersed in the BC network. Due

to the porous structure and high specific surface area in the range of 150-201 m²/g, this product may be beneficial for supercapacitance applications.²¹

Atomic force microscopy (AFM) was used for the determination of absorption of RGO. For this specific end, wet purified BC/RGO composite film was placed on mica disk and then later air-dried. It is widely known that bacterial cellulose possesses a random nanofibrillar structure.⁴³ From the AFM images, (Figure 5 h,i,j) the topography, phase change, and 3D topography image of BC/RGO composite film can be seen. It can be readily ascertained that the incorporation of RGO in the culture media did NOT influence the BC nanofibrous structure. From the phase change image, it can be observed that the RGO sheets are randomly embedded inside the BC network. The RGO sheets assembled each other into larger sheets because of the agitated motion of the entire culture medium. The RGO sheets may be attached by hydrogen bonding between the hydroxyl groups of cellulose and the surfaces of the RGO sheets. At high concentrations of RGO, a jet black sheet of BC/RGO formed, and encapsulated the entire composite (see Figure 5c) which showed that RGO has strong affinity to BC and also with other RGO sheets. This kind of structure may have future application in binder-free lithium ion batteries as anode materials (see Figure 5h inset) by incorporating nanoparticles such as tin-dioxide, silicon, etc.⁴⁴

Conclusions

In conclusion, a highly novel, versatile, environmentally-friendly, and economically feasible method is introduced to reduce GO utilizing bacterial cellulose culture media. In addition, an *in-situ* biosynthesis method is proposed for producing three different kinds of BC/RGO composites: gelatinous sealed packets, BC/RGO composite aerogels, and composite films. The novel structures of the materials are conjectured to have potential applications in diffusion- controlled release of biocompounds, super capacitors, and lithium ion batteries in addition to potential areas. This work offers an inexpensive, simple, and potentially significant protocol to generate biocompatible cellulose-based nanoelectronic devices for use as flexible electronics in a number of biomedical applications that include nerve cell signaling, muscle cell actuation, and heart cell innervation.

Experimental Section

In-situ biosynthesis process: The BC/RGO composites were produced by the *Gluconacetobacter xylinus* (ATCC 10245) bacterial strain in mannitol culture medium containing yeast (0.5%), bacto-peptone (0.3%), D-mannitol (2.5%)⁴⁵ and GO dissolved in de-ionized water having initial pH of 6.5. Four different culture solutions (30 mL) with final concentrations of were used: GO 0.05 mg/mL (sample 1), 0.1 mg/mL (sample 2), 0.15 mg/mL (sample 3), 0.5 mg/mL (sample 4). The culture solutions were autoclaved at 121°C for 15 min, and a black RGO precipitation was formed during the process. To fully disperse the newly-formed RGO, the solutions were magnetically stirred for 1 hour and sonicated for another 1 hour. Then the solutions were autoclaved again to remove any possible contamination, followed by gentle sonication for 3-5 min until uniform solutions were

obtained. For the main culture, all the cells were pre-cultured in a test tube for two days at 110 rpm @ 30°C to maximize the number of bacteria for the main inoculation. The small pellicle formed in the test tube was inoculated into a 125 ml Erlenmeyer flask containing 30 ml of culture medium and RGO. Main cultivations were carried out @ 30°C for 7 days under agitated conditions at 110 rpm. The samples obtained were washed in a 1N NaOH solution at 80°C for 1 hour to dissolve the bacteria followed by repeated washing with de-ionized water until the sample had neutral pH according to the standard procedure,²³ and storage in de-ionized water for future usage and characterization. All wet samples were transferred into a polypropylene tube having the approximate dimensions of 10 mm diameter × 40 mm height and followed by freeze-drying to obtain 3D graphene-based aerogels.

Characterization: AFM measurements were performed with a Bruker Dimension 3000 in tapping mode. In general, a liquid droplet sample of GO dispersed in water, RGO dispersed in the culture medium, and a purified BC/RGO composite film were placed on freshly cleaved mica substrates and then dried by oven. The measurements were all performed in air at ambient temperature and pressure.

The ATR-FTIR spectra were obtained using a Perkin Elmer Frontier FTIR spectrometer. Scans were completed between 4000- 400 cm⁻¹ with 16 convolutions and a resolution of 4 cm⁻¹. A total of 64 scans were completed for each sample. The baselines of all the samples were corrected and analyzed using Omnic software.

X-Ray Photoelectron Spectroscopy (XPS) measurements were conducted on PHOIBOS 150 analyzer using dual anode monochromated Al/Ag radiation. The RGO was washed filtered and washed several times before analyzation. The pure GO sample was used for XPS measurement without any treatment.

Raman spectra were recorded from 1000-2000 cm⁻¹ on a Renishaw Raman microscope. The laser used has a wavelength of 514 nm and a spot size of ~1-2 μm. GO and purified RGO films were used for the Raman analysis.

Ultraviolet-visible (UV-vis) spectra were obtained using a Varian Cary 300 UV-Vis spectrometer. De-ionized water was used as the reference for the aqueous suspension of GO and RGO samples, and the culture medium was used as the reference for the suspension of GO and RGO dispersed in culture medium.

Scanning electron microscope of freeze-dried samples of BC/RGO composites were analyzed using an FEI Phenom. Cylindrical samples were cut cross-sectionally and longitudinally (along the length of sample) The samples were mounted on a metal stub and were coated using a gold sputter machine with a layer of gold approximately 100 Å thick to reduce charge interruptions. Samples were viewed at magnification between 5,000-20,000 × their original sizes. Revolution software and ImageJ software were used to deconvolute the SEM images and thereby analyze the surface morphology and cross sectional images of the BC/RGO composites.

Notes and references

¹¹⁰ *a* Fiber and Polymer Science Program, North Carolina State, 2820 Faucette Drive, Campus Box 8005, Raleigh, NC 27695, USA. Fax: (+1) 919 515 6302; Tel: (+1) 919 515 7707; E-mail: lalucia@ncsu.edu

^b Key Laboratory of Eco-Textiles, Ministry of Education, Jiangnan University, 1800 Lih Avenue, Wuxi, Jiangsu Province, Wuxi 214122, China.

† Electronic Supplementary Information (ESI) available: [details of any supplementary information available should be included here]. See DOI: 10.1039/b000000x/

‡ The authors acknowledge the use of the Analytical Instrumentation Facility (AIF) at North Carolina State University, which is supported by the State of North Carolina and the National Science Foundation. The authors thank Dr. Yuntian Zhu for the use of Raman microscope. In addition, the generous support of USB Cooperative Agreement 2012-2072/2432 for partial support of this work and the State Scholarship Fund from China Scholarship Council is cheerfully acknowledged. A.G.Nandgaonkar. and Q.Q.Wang. contributed equally in carrying out the experiments, analyzing the results, and writing the manuscripts.

- 1 A. K. Geim, K. S. Novoselov, *Nat. Mater.* 2007, **6**, 183-191.
- 2 C. Ji, M. Xu, S. Bao, C. Cai, Z. Lu, H. Chai, F. Yang, H. Wei, *J. Colloid Interface Sci.* 2013, **407**, 416-424.
- 3 Z. Chen, W. Ren, L. Gao, B. Liu, S. Pei, H. Cheng, *Nat Mat.* 2011, **10**, 424-428.
- 4 H. Hu, Z. Zhao, W. Wan, Y. Gogotsi, J. Qiu, *Adv Mater.* 2013, **25**, 2219-2223.
- 5 C. J. Docherty, C. Lin, H. J. Joyce, R. J. Nicholas, L. M. Herz, L. Li, M. B. Johnston, *Nat Commun.* 2012, **3**, 1228.
- 6 Y. Zhou, Q. Bao, L. A. L. Tang, Y. Zhong, K. P. Loh, *Chem Mater.* 2009, **21**, 2950-2956.
- 7 X. Gui, J. Wei, K. Wang, A. Cao, H. Zhu, Y. Jia, Q. Shu, D. Wu, *Adv Mater.* 2010, **22**, 617-621.
- 8 X. Li, J. Chen, X. Wang, M. E. Schuster, R. Schlögl, M. Antonietti, *ChemSusChem* 2012, **5**, 642-646.
- 9 H. Zhang, X. Zhang, X. Sun, D. Zhang, H. Lin, C. Wang, H. Wang, Y. Ma, *ChemSusChem* 2013, **6**, 1084-1090.
- 10 D. Chen, L. Li, L. Guo, *Nanotechnology* 2011, **22**, 325601.
- 11 J. Gao, F. Liu, Y. Liu, N. Ma, Z. Wang, X. Zhang, *Chem Mater.* 2010, **22**, 2213-2218.
- 12 J. Liu, S. Fu, B. Yuan, Y. Li, Z. Deng, *J. Am. Chem. Soc.* 2010, **132**, 7279-7281.
- 13 F. Yang, Y. Liu, L. Gao, J. Sun, *J Phys Chem C.* 2010, **114**, 22085-22091.
- 14 Y. Wang, Z. Shi, J. Yin, *ACS App. Mater Inter.* 2011, **3**, 1127-1133.
- 15 N. Petersen, P. Gatenholm, *Appl. Microbiol. Biotechnol.* 2011, **91**, 1277-1286.
- 16 B. Malcolm, Microbial Cellulose: A New Resource for Wood, Paper, Textiles, Food and Specialty Products
<http://www.botany.utexas.edu/facstaff/facpages/mbrown/position1.htm>, May, 2013.
- 17 H. Liang, Q. Guan, L. S. Zhu-Zhu, H. Yao, X. Lei, S. Yu, *NPG Asia Mater.* 2012, **4**, e19.
- 18 B. Wang, X. Li, B. Luo, J. Yang, X. Wang, Q. Song, S. Chen, L. Zhi, *Small* 2013, **9**, 2399-2404.
- 19 M. Wang, I. V. Anoshkin, A. G. Nasibulin, J. T. Korhonen, J. Seitsonen, J. Pere, E. I. Kauppinen, R. H. Ras, O. Ikkala, *Adv Mater.* 2013, **25**, 2428-2432.
- 20 Z. Wu, C. Li, H. Liang, J. Chen, S. Yu, *Angew Chem.* 2013, **125**, 2997-3001.
- 21 W. Ouyang, J. Sun, J. Memon, C. Wang, J. Geng, Y. Huang, *Carbon.* 2013, **62**, 501-509.
- 22 Y. Feng, X. Zhang, Y. Shen, K. Yoshino, W. Feng, *Carbohydr. Polym.* 2012, **87**, 644-649.
- 23 Z. Yan, S. Chen, H. Wang, B. Wang, J. Jiang, *Carbohydr. Polym.* 2008, **74**, 659-665.
- 24 W. Park, H. Kim, S. Kwon, Y. Hong, H. Jin, *Carbohydr. Polym.* 2009, **77**, 457-463.
- 25 F. Wesarg, F. Schlott, J. Grabow, H. Kurland, N. Heßler, D. Kralisch, F. A. Müller, *Langmuir* 2012, **28**, 13518-13525.
- 26 S. Yano, H. Maeda, M. Nakajima, T. Hagiwara, T. Sawaguchi, *Cellulose* 2008, **15**, 111-120.
- 27 G. Yamal, P. Sharmila, K. Rao, P. Pardha-Saradhi, *Process Biochem.* 2013, **48**, 532-538.
- 28 G. Yamal, P. Sharmila, K. Rao, P. Pardha-Saradhi, *PLoS one.* 2013, **8**, e61750.
- 29 E. T. Sayed, Y. Saito, T. Tsujiguchi, N. Nakagawa, *J. Biosci. Bioeng.* 2012, **114**, 521-525.
- 30 M. Masuda, S. Freguia, Y. Wang, S. Tsujimura, K. Kano, *Bioelectrochemistry* 2010, **78**, 173-175.
- 31 Y. Xu, H. Bai, G. Lu, C. Li, G. Shi, *J. Am. Chem. Soc.* 2008, **130**, 5856-5857.
- 32 B. Baêta, S. Aquino, S. Silva, C. Rabelo, *Biodegradation* 2012, **23**, 199-208.
- 33 J. Paredes, S. Villar-Rodil, M. Fernandez-Merino, L. Guardia, A. Martinez-Alonso, J. Tascon, *J. Mater. Chem.* 2011, **21**, 298-306.
- 34 W. Chen, L. Yan, P. R. Bangal, *Carbon* 2010, **48**, 1146-1152.
- 35 T. Szabó, O. Berkesi, P. Forgó, K. Josepovits, Y. Sanakis, D. Petridis, I. Dékány, *Chem Mater.* 2006, **18**, 2740-2749.
- 36 A. Ferrari, J. Robertson, *Phys. Rev. B.* 2000, **61**, 14095.
- 37 H. Wang, J. T. Robinson, X. Li, H. Dai, *J. Am. Chem. Soc.* 2009, **131**, 9910-9911.
- 38 D. Mhamane, W. Ramadan, M. Fawzy, A. Rana, M. Dubey, C. Rode, B. Lefez, B. Hannoyer, S. Ogale, *Green Chem.* 2011, **13**, 1990-1996.
- 39 D. R. Ruka, G. P. Simon, K. M. Dean, *Carbohydr. Polym.* 2012, **89**, 613-622.
- 40 F. Yoshinaga, N. Tonouchi, K. Watanabe, *Biosci. Biotechnol. Biochem.* 1997, **61**, 219-224.
- 41 M. Schramm, S. Hestrin, *J. Gen. Microbiol.* 1954, **11**, 123-129.
- 42 W. Czaja, D. Romanovicz, R. Malcolm Brown, *Cellulose* 2004, **11**, 403-411.
- 43 B. Surma-Ślusarska, S. Presler, D. Danielewicz, *Fibers Text East Eur.* 2008, **16**, 69.
- 44 E. G. Bae, Y. Hwang, M. Pyo, *Bull.KoreanChem.Soc.* 2013, **34**, 1199.
- 45 T. Oikawa, T. Ohtori, M. Ameyama, *Biosci. Biotechnol. Biochem.* 1995, **59**, 331-332.